The concentration, source and deposition flux of inorganic nitrogen in atmospheric particles during dust events at a coastal site in northern China

Jianhua Qi[1], Xiaohuan Liu[1], Xiaohong Yao[1], Ruifeng Zhang[1], Xiaojing Chen[1], Xuehui Lin[2], Huiwang Gao[1], Ruhai Liu[1]

[1]Key Laboratory of Marine Environment and Ecology, Ministry of Education, Ocean University of China, Qingdao, 266100, China

[2]Qingdao Institute of Marine Geology, Qingdao, 266100, China

Correspondence to: Jianhua Qi (qjianhua@ouc.edu.cn)

Abstract. Asian dust has been reported to carry anthropogenic reactive nitrogen during transport from source areas to the oceans. In this study, we attempted to characterize NH_4^+ and NO_3^- in atmospheric particles collected at a coastal site in northern China during spring dust events from 2008 to 2011. Based on the mass concentrations of NH_4^+ and NO_3^- in each total suspended particle (TSP) sample, the samples can be classified into increasing or decreasing types. In Category 1, the concentrations of NH_4^+ and NO_3^- were 20%-440% higher in dust day samples relative to samples collected immediately before or after a dust event. These concentrations decreased by 10-75% in the dust day samples in Categories 2 and 3. Back trajectory analysis suggested that multiple factors such as the transport distance prior to the reception site, the mixing layer depth on the transport route and the residence time across highly polluted regions, might affect the concentrations of NH_4^+ and NO_3^-. NH_4^+ in the dust day samples was likely either in the form of ammonium salts existing externally with dust aerosols or as the residual of incomplete reactions between ammonium salts and carbonate salts. NO_3^- in the dust day samples was attributed to various formation processes during the long-range transport. The positive matrix factorization (PMF) receptor model results showed that the contribution of soil dust increased from 23% to 36% (90% of the residuals<3.0 and r^2=0.97) on dust days with decreasing contributions from local anthropogenic inputs and associated secondary aerosols. The estimated deposition flux of inorganic nitrogen varied greatly from event to event, e.g., the dry deposition flux of particulate inorganic nitrogen increased by 9-285% in Category 1, but decreased by 46%-73% in Category 2.

Keywords: aerosols, nitrogen, dust, source apportionment, dry deposition flux

1 Introduction

Reactive nitrogen carried in dust particles can be transported over a long distance, and the atmospheric nitrogen deposition in oceans has been recognized as an important external source of the nitrogen supporting phytoplankton growth (Duce et al., 2008; Zhang et al., 2010b). This hypothesis has been evaluated through incubation experiments, in situ experiments, and the use of satellite observational data (Banerjee and Kumar 2014; Guo et al., 2012; Liu et al., 2013; Shi et al., 2012; Tan and Wang, 2014). However, the process is dynamic due to the worldwide changing emissions of NO_x and NH_3 in the last few decades. For example, China and most of the developing countries in Asia experienced a large increase in emissions of NH_3 and NO_x while a substantial decrease in emissions occurred in Europe over the last three decades (Grice et al., 2009; Liu et al., 2017; Ohara et al., 2007; Skjøth and Hertel, 2013). The change would affect the nitrogen carried by dust particles to some extent, and updated studies are thereby essential.

Asian dust is one of three largest dust sources on earth. Asian dust has been reported to not only frequently cross over the mainland and the China Seas, but also to occasionally reach the remote northern Pacific Ocean or North America (Creamean 2013; Tan and Wang, 2014; Van Curen and Cahill, 2002; Zhang and Gao, 2007). In an extreme case, Asian dust was found to be transported more than one full circuit around the globe in approximately 13 days (Uno et al 2009). During the long-range transport, dust particles may mix with anthropogenic air pollutants and consequently undergo complicated chemical reactions (Cui et al., 2009; Li et al., 2014; Ma et al., 2012; Wang et al., 2011; Wang et al., 2016; Wang et al., 2017a; Xu et al., 2014; Yang et al., 2002). For example, a few studies have shown that the concentrations of atmospheric particulate NO_3^- and NH_4^+ on dust storm days were 2-5 times larger than those prior to the events in Beijing (Liu et al., 2014; Liu and Bei, 2016). Fitzgerald et al. (2015) found that almost all Asian dust events observed in Korea contained considerable amounts of nitrate. However, Zhang et al. (2010a) reported an interesting result, i.e., the stronger dust storms corresponded to the smaller increases in these ions. This raises the complex for carrying reactive nitrogen by dust particles.

A few contradictory results were also reported in the literature, which made the scientific issue even

more complicated. For example, the concentration of NO_3^- in atmospheric aerosols on dust days was significantly lower in comparison to the concentration measured immediately before or after the event at a rural site in Yulin near the Asian dust source region (Wang et al., 2016). The phenomenon was also observed in Shanghai, a mega city at a few thousands of kilometers from dust source zones in China, and more downwind sites (Kang et al., 2013; Li et al., 2014; Wang et al., 2013).

To update and improve our knowledge on reactive nitrogen carried by dust particles, we collected atmospheric aerosol particles during and prior to (or post, but only when no sample was collected prior to dust events) at a coastal site adjacent to the Yellow Sea in each spring of 2008-2011. The concentrations of inorganic nitrogen and other components were determined for analysis. In this study, we first characterized the concentrations of inorganic nitrogen in dust samples by comparing them with the values in atmospheric particles measured either prior to or post the event. We then conducted source apportionment to quantify their sources. Finally, we calculated and discussed the deposition flux of atmospheric particulate inorganic nitrogen during dust events.

2 Experimental methods

2.1 Sampling

Fig. 1 shows the sampling site, which is situated at the top of a coastal hill (Baguanshan) in Qingdao in northern China (36 ° 6' N, 120 ° 19' E, 77 m above sea level) and is approximately 1.0 km from the Yellow Sea to the east. A high-volume air sampler (Model KC-1000, Qingdao Laoshan Electronic Instrument Complex Co., Ltd., China) was set up on the roof of a two-story office building to collect total suspended particle (TSP) samples on quartz microfiber filters (Whatman QM-A) at a flow rate of 1 m^3/min. Prior to sampling, the filters were heated at 450 ℃ for 4.5 hrs to remove organic compounds. Our sample collection strategy involved collecting dust samples representing long-range transported particles. We followed the definition of dust events adopted in the regulations of surface meteorological observations of China (CMA, 2004; Wang et al., 2008) and identified dust events based on the meteorological records (Weather Phenomenon) of Qingdao from the Meteorological Information Comprehensive Analysis and Process System (MICAPS) of the China Meteorological Administration. Due to no dust events lasting over 12 hrs (Lee et al., 2015; Su et al., 2017; Zhang et al., 2007), we collected one dust sample with a 4-hr duration in a day. The sampling for dust particles started only

when the measured PM_{10} mass concentration in Qingdao (http://www.qepb.gov.cn/m2/) and the forecasted dust mass over Asia (http://www-cfors.nies.go.jp/~cfors/) had greatly increased.

On March 20-21, 2010, two dust events subsequently swept Qingdao. The 4 hr dust samples with IDs of 20100320 and 20100321 may not capture the entirety of the two events. However, the on-line data can allow adequate separation of the two dust event samples. The same was true for the dust samples with IDs of 20110501, 20110502. Table 1 lists the sampling information. Based on the forecast, we also collected aerosol particle samples immediately before, which were regarded as the reference samples. These reference samples were further classified into sunny day samples and cloudy day samples. For those events missing sampling prior to dust events, we collected post-dust samples under clear and sunny weather conditions as early as possible.

Asian dust events were mostly observed in the spring at the sampling site. Our intensive samplings were concentrated in the period of March to May in 2008-2011, when a smaller outbreak for Asian dust events was observed in northern China (Fig. S3). Overall, a total of 14 sets of dust samples and 8 sets of comparison samples were available for analysis in this study.

To facilitate the coastal sampling data analysis, sand samples were collected at the remote site of Zhurihe (42 °22'N, 112 °58'E) in the Hunshandake Desert, one of the main Chinese sand deserts, in April 2012. Sand samples were packed in clean plastic sample bags and were stored below -20 ℃ before the transfer. An ice-box was used to store the samples during transport to the lab for chemical analysis.

2.2 Analysis

The aerosol samples were weighted according to the standard protocol. The sample membranes were then cut into several portions for analysis. One portion of each aerosol sample was ultrasonically extracted with ultra-pure water in an ice water bath for determining inorganic water-soluble ions using ICS-3000 ion chromatography (Qi et al., 2011). The sand samples collected at the Zhurihe site were analyzed using the same procedure. We later refer to dissolved inorganic nitrogen (DIN) as the sum of nitrate and ammonium by excluding nitrite because of its very low concentration.

One portion of the each aerosol filter was cut into 60 cm^2 pieces and digested with HNO_3+$HClO_4$+HF (5:2:2 by volume) at 160 ℃ using an electric heating plate. The concentrations of Cu, Zn, Cr, Sc and Pb were measured using inductively coupled plasma mass spectrometry (Thermo X Series 2), while the concentrations of Al, Ca, Fe, Na and Mg were measured using inductively coupled

plasma atomic emission spectroscopy (IRIS Intrepid II XSP). Field blank membranes were also analyzed for correction.

One portion of aerosol sample was digested with an HNO_3 solution (10% HNO_3, 1.6 M) at 160 ℃ for 20 min in a microwave digestion system (CEM, U.S.). The Hg and As in sample extracts were analyzed following the U.S. Environmental Protection Agency method 1631E (U.S. EPA, 2002) using cold vapor atomic fluorescence spectrometry (CVAFS). The detection limits, precisions and recoveries of water-soluble ions and metal elements are listed in Table 2.

2.3 Computational modeling

The enrichment factor of metal elements was given by

$$EF_i = \frac{\left(X_i / X_{\mathrm{Re}}\right)_{aerosols}}{\left(X_i / X_{\mathrm{Re}}\right)_{crust}} \quad (1)$$

where subscripts *i* and *Re* refer to the studied metal and the reference metal, respectively; $(X_i/X_{Re})_{aerosols}$ is the concentration ratio of metal *i* to metal *Re* in the aerosol samples; and $(X_i/X_{Re})_{crust}$ is the ratio of metal *i* to metal *Re* in the Earth's crust. For the calculation of the enrichment factor of the metal elements, scandium was used as the reference element (Han et al., 2012), and the abundance of elements in the Earth's crust given by Taylor (1964) was adopted.

The 72-h air mass back trajectories were calculated for each TSP sample using TrajStat software (Wang et al., 2009) and National Oceanic and Atmospheric Administration (NOAA) GDAS (Global Data Assimilation System) archive data (http:// www.arl.noaa.gov/ready/hysplit4.html). The air mass back trajectories were calculated at an altitude of 1500 m to identify the dust origin. In addition, the distance over sea of the air mass for each sample was measured from the trajectory using TrajStat software (Wang et al., 2009).

The positive matrix factorization (PMF) is a commonly used receptor modeling method. This model can quantify the contribution of sources to samples based on the composition or fingerprints of the sources (Paatero and Tapper, 1993; Paatero, 1997). The measured composition data can be represented by a matrix X of *i* by *j* dimensions, in which *i* number of samples and *j* chemical species were measured, with uncertainty *u*. *X* can be factorized as a source profile matrix (*F*) with the number of source factors (*p*) and a contribution matrix (*G*) of each source factor to each individual sample, as shown in Equation 2.

$$X_{ij} = \sum_{k=1}^{p} G_{ik} F_{kj} + E_{ij} \quad (2)$$

where E_{ij} is the residual for species j of the i-th sample.

The aim of the model is to minimize the objective function Q, which was calculated from the residual and uncertainty of all samples (Equation 3), to obtain the most optimal factor contributions and profiles.

$$Q = \sum_{i=1}^{n} \sum_{j=1}^{m} (E_{ij}/u_{ij})^2 \quad (3)$$

The EPA PMF 3.0 model was used to obtain the source apportionment of atmospheric particulates on dust and comparison days. The correlation coefficient between the predicted and observed concentrations was 0.97.

Dry deposition velocities were obtained using Williams' model (Williams, 1982) by accounting for particle growth (Qi et al., 2005). Williams' model is a two-layer model used to calculate the dry velocity of size-segregated particles over the water. In an upper layer below a reference height (10 m), the deposition of aerosol particles is governed by turbulent transfer and gravitational settling. In the deposition layer, the gravitational settling of particles is affected by particle growth due to high relative humidity. To obtain the deposition velocity of different particle sizes, Williams' model needs many input parameters, such as the wind speed at 10-m height (U_{10}), air/water temperature, and relative humidity. Relative humidity, air temperature and U_{10} from the National Centers for Environmental Prediction (NCEP) were used in this study. Surface seawater temperature data was collected from the European Centre for Medium-Range Weather Forecasts (ECMWF). The meteorological and seawater temperature data had a six-hour resolution. According to a previously reported method (Qi et al., 2013), the dry deposition fluxes of the particles and the nitrogen species were calculated for dust and comparison days.

The CMAQ model (v5.0.2) was applied over the East Asia area to simulate the concentrations of PM10, NO_x and NH_3 for 14 samples collected during 11 dust events. The simulated domain contains 164×97 grid cells with a 36-km spatial resolution, and the centered point was 110 °E, 34 °N. The vertical resolution includes 14 layers from the surface to the tropopause, with the first model layer at a height of 36 m above the ground level. The meteorological fields were generated by the Weather Research and Forecasting (WRF) Model (v3.7). Considering that the simulated area is connected to the Yellow Sea, the CB05Cl chemical mechanism was chosen to simulate the gas-phase chemistry. The emissions of NO_X and NH_3 over East Asia for each dust event were also modeled using the CMAQ model according

to the emission inventory in 2008, which was generated by extrapolating the 2006 activity data to the year 2008 using the method described by Zhang et al. (2009). Initial conditions (ICONs) and boundary conditions were generated from a global chemistry model of GEOS-CHEM. All the dust events simulations are performed separately, each with a 1-week spin-up period to minimize the influence of the ICONs. The validation of the application of the CMAQ model in China has been reported by Liu et al. (2010a, b).

2.4 Other data sources and statistical analysis

Meteorological data were obtained from the Qingdao Meteorological Administration (http://qdqx.qingdao.gov.cn/zdz/ystj.aspx) and the MICAPS of the Meteorological Administration of China. Different weather characteristics, such as sunny days, cloudy days and dust days, were defined according to information from the MICAPS and Qingdao Meteorological Administration. According to the altitude, longitude and latitude of the 72-hr air mass back trajectory of each dust sample, the pressure level, temperature and relative humidity (RH) data along the path of the air mass were derived from the NCEP/NCAR re-analysis system (http://www.esrl.noaa.gov/psd/data/gridded/data.ncep.reanalysis.html) for each sample. The mixed layer depth during the air mass transport of dust samples was obtained from the HYSPLIT Trajectory Model (http://ready.arl.noaa.gov/hypub-bin/trajasrc.pl) using the same method. Then the average mixing layer, transport altitude, air temperature and RH were calculated as an average of all points on the air mass back trajectory of each sample. Spearman correlation analysis was applied to examine the relationships of nitrate and ammonium with transport parameters, and P values of <0.05 were considered to be statistically significant.

3 Results

3.1 Characterization of aerosol samples collected during dust events

We first examined the mass concentrations of TSP samples and the concentrations of crustal and anthropogenic metals therein through a comparison with the reference samples collected on dust days and immediately before or after days, providing the background information for our target species analyzed later. The comparative results are highlighted below. For these reference samples, the TSP mass concentrations ranged from 94 to 275 $\mu g \cdot m^{-3}$, with an average of 201 $\mu g \cdot m^{-3}$ (Fig. 2, Table S1).

The TSP mass concentration increased substantially to 410-3857 $\mu g \cdot m^{-3}$ in dust day samples, with an average of 1140.3 $\mu g \cdot m^{-3}$. In each pair of dust day sample against reference sample, the net increase in the mass concentration of TSPs was 82-1,303%, with a median value of 403% (Table S1). A similar increase was present in the crustal elements in each pair of samples. For example, the mean concentrations of Sc, Al, Fe, Mg and nss-Ca (usually used as a typical dust index) increased by more than a factor of two. On the other hand, the enrichment factors (EF) of Al, Fe, Ca, and Mg were less than three in dust day samples with values less than 14 in the reference samples (Table 3). Lower values are indicative of elements from a primarily crustal origin. The average mass concentrations of anthropogenic elements, such as Cu, Pb, Zn, Cr, Hg and As, in dust day samples increased by 107% to 722% against those in the reference sample; however, the EF of the anthropogenic metal elements decreased in the former. This indicates that dust particles likely carried more anthropogenic elements, although their relative contribution to the total mass was lower than that in the reference sample. Note that Sample 20110415 was excluded for further analysis. It was judged as a local blowing dust event because no corresponding dust event existed upwind.

3.2 Concentrations of inorganic nitrogen in dust day samples

When the mass concentrations of NH_4^+ and NO_3^- in each pair of TSP samples were compared, the concentrations of NH_4^+ increased by 8%-473% in some dust day samples (20080301, 20080315, 20090316, 20100315, 20100320, 20100321, 20110418 and 20110502), but decreased by 28-84% in other dust day samples (Fig. 3, Column NH_4^+ and NO_3^- in Table S1). The same was generally true for the measured concentrations of NO_3^-.

Considering the relative values of NH_4^+ and NO_3^- in dust day samples relative to the reference samples, we classified the dust day samples into three categories (Table 4). In Category 1, the mass concentrations of NH_4^+ and NO_3^- were larger in dust day samples against the reference samples. In Category 2, the reverse was true. In Category 3, the mass concentrations of NO_3^- were lower in the dust samples than in the reference samples, whereas the concentrations of NH_4^+ were close to the reference. As reported, the Yellow Sea encountered dust storms mainly derived from the Hunshandake Desert (Zhang and Gao, 2007). We thereby compared our observations with the sand particles collected from this desert (Table 5). The ratios of mass concentrations of nitrate and ammonium to the total mass of sand particles were very low, i.e., less than 81 μg/g, which are approximately three orders of magnitude

less than the corresponding values in our dust samples. The values obtained from atmospheric aerosols at the urban sites of Duolun (Cui, 2009) and Alxa Right Banner (Niu and Zhang, 2000), which are closer to the desert, increased on dust days, but were still over one order of magnitude lower than the corresponding values in this study (Table 5). The mixing and chemical interaction between anthropogenic air pollutants and dust particles during transport from the source zone to the reception site likely played an important role in increasing the ratios, leading to extremely larger ratio values at this site relative to those in source dust and in upwind atmospheric particles (Cui et al., 2009; Wang et al., 2011; Wu et al., 2016). However, the increase or decrease in the mass concentration absolute of nitrate and ammonium in different dust samples against the reference implied the complex for the interactions.

4. Discussion and conclusion

4.1 Theoretical analysis of the three categories

Ammonium salts are common in atmospheric particles with diameters of less than 2 μm (Yao et al., 2003; Yao and Zhang, 2012). Many modeling studies have shown that the gas-aerosol thermodynamic equilibrium is assumed to be fully attained for inorganic ions, including ammonium salts in $PM_{2.5}$ (Dentener et al., 1996; Underwood et al., 2001; Wang et al., 2017a; Zhang et al., 1994; Zhang and Carmichael, 1999). Reasonably good agreements between ammonium salt modeling results and observations reported in the literature support the validity of this assumption (Chen et al., 2016; Penrodet al., 2014; Walker et al., 2012). Supposing that a thermodynamic equilibrium had been attained by the ammonium salts in Category 1, the reactions between carbonate salts and ammonium salts, such as 1) $(NH_4)_2SO_4 + CaCO_3 \Rightarrow CaSO_4 + NH_3$ (gas) $+CO_2$ (gas) $+H_2O$ and 2) $2NH_4NO_3 + CaCO_3 \Rightarrow Ca(NO_3)_2 + 2NH_3$ (gas) $+CO_2$ (gas) $+H_2O$, will release NH_3 (gas) until $CaCO_3$ has been completely used up. During dust events, very high concentrations of Ca^{2+} were observed, and high $CaCO_3$ concentrations were therefore expected. For example, the single-particle characterization showed that Asia dust from the Gobi and Inner Mongolian Deserts had rich $CaCO_3$, with a ratio of 4.3-6.7% for reacted $CaCO_3$ and 3.0-4.6% for unreacted $CaCO_3$ (Hwang et al., 2008). Heterogeneous chemical reactions of mineral dust mostly occurred on $CaCO_3$ mineral dust (Hwang and Ro, 2006). However, when Category 1 was considered alone and one exterior sample was excluded, a good correlation was obtained for $[NH_4^+]_{\text{equivalent concentration}} = 0.98 * [NO_3^- + SO_4^{2-}]_{\text{equivalent concentration}}$ (R^2=0.83,

$P<0.05$). The good correlation, together with the slope of 1, strongly indicated that the NO_3^- and SO_4^{2-} were almost completely associated with NH_4^+ in these dust day samples. It was commonly believed that anthropogenic ammonium nitrate and ammonium sulfate were produced by gas, aqueous phase reaction and thermodynamic equilibrium processes, and this anthropogenic ammonium nitrate and ammonium sulfate was externally mixed with dust particles (Wang et al., 2017a). In reverse, the poor correlation of Ca^{2+} to NO_3^- and SO_4^{2-} showed that the formation of $CaSO_4$ and/or $Ca(NO_3)_2$ was probably negligible. Thus, ammonium salt aerosols may externally exist with dust aerosols in these dust day samples. Wang et al. (2017a) also found that coarse mode ammonium was quite low and fine mode dust particles were externally mixed with anthropogenic ammonium nitrate and ammonium sulfate. NO_3^- and NH_4^+ in Asia dust samples were argued to be more physically affected by the dust storm, i.e., the dilution effect, rather than the chemical reaction on the dust (Huang et al., 2010). The hypothesis appeared to be valid in Category 1, where NH_4^+ was negatively correlated with Ca^{2+} (Fig. S4). In the exterior sample collected on 21 March 2010, $[NH_4^+]$ only accounted for ~70% of the observed $[NO_3^-+SO_4^{2-}]$ in an equivalent concentration. This result suggested that ~30% of $(NO_3^-+SO_4^{2-})$ may be associated with dust aerosols via the formation of metal salts of the two species. This hypothesis was supported by the correlation result, i.e., NO_3^- was positively correlated with NH_4^+ and Cu, and SO_4^{2-} was correlated with K^+, Na^+ and Mg^{2+} (Fig. S4). Cu was once used as an effective marker of diesel and biodiesel-blend exhaust (Gangwar et al., 2012), while it can also be derived from copper pyrites ($CuFeS_2$) in Inner Mongolia mines (Huang et al., 2010). The increase of Cu in the mass concentration in dust samples implied dust particles mixed with anthropogenic particles, particularly from industrial emissions, during transport.

For Category 2, no correlation between $[NH_4^+]_{\text{equivalent concentration}}$ and $[NO_3^-+SO_4^{2-}]_{\text{equivalent concentration}}$ existed. When Category 2 was considered alone and one exterior sample was excluded, the equivalent ratios of NH_4^+ to $NO_3^-+SO_4^{2-}$ were generally much smaller than 1, suggesting that a larger fraction of $NO_3^-+SO_4^{2-}$ may exist as metal salts due to reactions of their precursors with dust aerosols. NO_3^- and SO_4^{2-} showed no correlations with NH_4^+ but did show significant correlations with Pb (Fig. S4). The average concentration of Ca^{2+} in Category 2 (0.43 ± 0.40 $\mu g/m^3$) was evidently higher than that in Category 1 (Ca^{2+}: 0.17 ± 0.04 $\mu g/m^3$), implying the probable formation of $CaSO_4$ and/or $Ca(NO_3)_2$ and the release of NH_3 (gas). Moreover, except for 20080502, the remaining dust samples in Category 2

were transported from the desert relatively enriched with $CaCO_3$ (1-25% in Wt%) (Formenti et al., 2011). A positive correlation between NO_3^- and SO_4^{2-} in Category 2 against a negative correlation in Category 1 also implied that the dust particles enriched with $CaCO_3$ in Category 2 might play an important role to form SO_4^{2-} and NO_3^-. Ca-rich dust particles coated with highly soluble nitrate were observed at Kanazawa in Japan during Asian dust storm periods using SEM/EDX (scanning electron microscopy equipped with an energy dispersive X-ray spectrometer) (Tobo et al.， 2010). The single-particle observation conducted by Hwang and Ro (2006) showed that $CaCO_3$ in dust particles was almost completely consumed to produce mainly $Ca(NO_3)_2$ species.

4.2 Source apportionment of aerosols during dust and non-dust events

The sources of atmospheric aerosols in dust and reference samples were determined by PMF modeling (Paatero and Tapper, 1993; Paatero, 1997). Fig. 4 shows that atmospheric aerosols in the reference samples mainly included six sources, i.e., industry, soil dust, secondary aerosols, sea salt, biomass burning, and coal combustion/other sources, with 90% of the scaled residuals falling between -3 and +3; r^2=0.97. In these dust samples, including Categories 1-3, oil combustion, industry, soil dust, secondary aerosols, and coal combustion/other sources were identified as five major sources (Table 6). The contribution of soil dust evidently increased from 23% to 36% in the dust samples relative to the reference, consistent with the high concentrations of TSPs and crustal metals observed on dust days. The calculated contribution of nitrate plus ammonium from the soil dust source to the total mass of nitrate plus ammonium in the dust samples greatly increased. The source profile for coal combustion in the dust day samples showed a high percentage of K^+, Cl^-, Ca, Mg, Co, Ni, As, Al and Fe, indicating that coal combustion particles may exist contemporaneously with other anthropogenic pollutants emitted along the transport path. Liu et al. (2014) also found a larger net increase in the contribution of dust aerosols to the mass of PM_{10}, i.e., 31%-40%, on dust days against non-dust days in Beijing which is approximately 600 km upwind of Qingdao. Accordingly, they reported that the contributions of local anthropogenic sources decreased on dust days, especially those from secondary aerosols, consistent with the EF of anthropogenic metals observed on dust days.

4.3 Influence of transport path ways on particulate inorganic nitrogen in dust samples

The calculated air mass trajectories for 13 out of 14 samples showed that the air mass originated

from North and Inner Mongolia, China (Fig. 5), generally consistent with the results of Zhang and Gao (2007). The remaining one, with ID of 20110418 originated from Northeast China. The calculated trajectories showed that the entire dust air mass passed over those highly polluted regions with strong emissions of NO_x and NH_3 shown in Fig 6 and experienced different residence times therein. Fig. 5 shows that all air mass trajectories in Category 1 were transported from either the north or northwest over the continent, except for the one exterior sample 20110502. In Category 2, the air masses always took a 94-255 km trip over the sea prior to arriving at the reception site. NH_3-poor conditions in the marine atmosphere disfavored the formation and existence of ammonium nitrate. On the other hand, the humid marine conditions (the average RH ranged in 50-75% over the Bohai and Yellow Seas in 2006-2012) might have enhanced hetero-coagulation between dust and smaller anthropogenic particles, leading to the release of NH_3 via reactions between preexisting ammonium salts and carbonate salts.

The average mixing layer was less than 900 m along the air mass transport routes for most sampling days in Category 1 (Table 7), favoring the trapping of locally emitted anthropogenic air pollutants in the mixing layer. The air masses in Category 1 took over 11-39 hrs to cross over the highly polluted area with appreciable concentrations of NO_x (5.7±1.4 ppb) and NH_3 (7.6±3.3 ppb). Except for the exterior samples, air masses in Category 2 took less than 10 hrs to cross over the polluted areas with lower concentrations of NO_x (3.6±3.4 ppb) and NH_3 (4.7±4.7 ppb) and the mixing layer height along the route was 916-1194 m (on average) for each dust event. Moreover, the averaged wind speed at sampling site was 2.8 m/s in Category 1, but 6.2 m/s in Category 2. The lower wind speed in Category 1 was unexpected, implying dust particles very likely traveled at aloft with a high speed and then mixed down to the ground through subsidence. This further led to the external mixing of anthropogenic particulate matters and dust. The correlation analysis results in Table S2 indirectly support these conclusions.

The concentrations of PM10 and its major components NO_3^- and NH_4^+ over East Asia on dust days and comparison days were modeled using the WRF-CMAQ model (Fig. S5-6). Spatial distributions of PM10 during each dust events were consistent with the records in the "Sand-dust Weather Almanac" (CMA, 2009; 2010; 2012; 2013). The dust particles were transported eastward by passing over the sampling site, the China Sea and arriving at the far remote ocean region, except for the local blowing dust sample with ID of 20110415, as mentioned previously. NMB (normalized mean bias) values of NO_3^- were -4% and -12% in dust and non-dust reference samples, respectively, indicating that CMAQ

results reasonably reproduce the mass concentrations of NO_3^- (Fig. S6). Simulated NH_4^+ concentrations in dust samples were severely under-predicted with NMB values at -71%. For reference samples, simulated NH_4^+ concentrations sometimes can well reproduce the observational values, but sometimes totally off. The external mixing mechanism proposed in this study is urgently needed to be included in the model for accurately predicting the concentrations during dust events.

4.4 Dry deposition fluxes of TSP, particulate inorganic nitrogen and metals

Dust events are known to increase the deposition fluxes of aerosol particles along the transport path because of high particle loadings. For example, Fu et al. (2014) found that the long-range transported dust particles increased the dry deposition of PM_{10} in the Yangtze River Delta region by a factor of approximately 20. In terms of atmospheric deposition in the oceans, a few studies reported enhancements in oceanic chlorophyll *a* following dust storm events (Banerjee and Kumar, 2014; Tan and Wang, 2014). In addition to those in high-nutrient and low-chlorophyll (HNLC) regions, the input of nitrogen and other nutrients associated with dust deposition is expected to promote the growth of phytoplankton in oceans with varying nutrient limitation conditions. Thus, we calculated the dry deposition fluxes of aerosols particles, $N_{NH4+NO3-}$ and metal elements during dust and reference periods using the measured component concentrations and modeled dry deposition velocities (Table 8). We also compared the calculated dry deposition flux of TSP and $N_{NH4+NO3}$- with previous observations in the literature.

The dry deposition fluxes of atmospheric particulates increased on dust days against the reference to some extent. For example, the particle deposition fluxes varied over a wide range from 5,200 to 65,000 mg/m^2/month in different dust sampling days, with an average of 18,453 mg/m^2/month, in comparison with the dry deposition flux of TSP of 2,800±700 mg/m^2/month from the reference periods in the coastal region of the Yellow Sea. The dry deposition fluxes of $N_{NH4+NO3}$- varied, depending on Category 1, 2 or 3. In Category 1, the dry deposition fluxes of $N_{NH4+NO3}$- increased by 9-75% with increased TSP flux by 86-252% (Table S3). In Categories 2 and 3, the dry deposition fluxes of TSP increased by 126% to 2,226% against the references. Excluding ammonium in Category 3, the dry deposition fluxes of particulate $N_{NH4+NO3}$- decreased by 44% (on average). A larger decrease in the concentration of nitrate was present in Categories 2 and 3, i.e., decreases of 73% and 46%, respectively. Note that the average ammonium deposition flux decreased by 47% in Category 2 but increased by 10%

in Category 3.

Except for Pb and Zn in Category 2, the dry deposition fluxes of Cu, Pb and Zn increased with those of nitrogen on dust days. Trace metals were found to have a toxic effect on marine phytoplankton and inhibit their growth (Bielmyer et al., 2006; Echeveste et al., 2012). Liu et al. (2013) found that inhibition coexisted with the promotion of phytoplankton species in incubation experiments in the southern Yellow Sea in the spring of 2011 by adding Asian dust samples to collected seawater. However, the dry atmospheric deposition fluxes of Fe increased by a factor of 124-2,370% in dust day samples. Wang et al. (2017b) recently reported that Fe can alleviate the toxicity of heavy metals. Moreover, atmospheric inputs of iron to the ocean have been widely proposed to enhance primary production in HNLC areas (Jickells et al., 2005).

Due to anthropogenic activity and economic development, inorganic nitrogen emissions increased in China from 1980 to 2010 (Fig. S3). The dry deposition flux of $N_{NH4+NO3}$- should have theoretically increased with the increase in the emission of inorganic nitrogen. Considering the different dry deposition velocities to be used in various studies, we recalculated the dry deposition flux of $N_{NH4+NO3}$- in the literature using the dry deposition velocities of 1 cm/s for nitrate and 0.1 m/s for ammonium, as reported by Duce et al. (1991). We thereby found that dry deposition fluxes of $N_{NH4+NO3}$- over the Yellow Sea during the dust days increased greatly from 1999 to 2007, but the values in Qingdao varied narrowly within a range of 94.75-99.65 mg N/m^2/month during the dust days from 1997 to 2011 (Table 9). The complicated results implied that even more updated works are needed in the future.

Acknowledgments. This work was supported by the Department of Science and Technology of the P. R. China through the State Key Basic Research & Development Program under Grant No. 2014CB953701 and the National Natural Science Foundation of China (No. 41375143). We thank Prof. Yaqiang Wang and Jinhui Shi for the valuable discussion regarding this research. We also express our appreciation to Tianran Zhang for help with sand sampling, and Qiang Zhang, Yang Yu and Jiuren Lin for data collection.

References

Banerjee, P., and Kumar, P. S.: Dust-induced episodic phytoplankton blooms in the Arabian Sea during winter monsoon, J. Geophys. Res-Oceans., 119, 7123-7138, 2014.

Bielmyer, G. K., Grosell, M., and Brix, K. V.: Toxicity of silver, zinc, copper, and nickel to the copepod

406 Acartia tonsa exposed via a phytoplankton diet, Environ. Sci. technol., 40, 2063-2068, 2006.
407 Chen, D., Liu, Z. Q., Fast, J., and Ban, J. M.: Simulations of sulfate–nitrate–ammonium (SNA)
408 aerosols during the extreme haze events over northern china in october 2014, Atmos. Chem. Phys.,
409 16, 10707-10724, 2016.
410 CMA: Regulations of Surface Meteorological Observation, China Meteorological Press, Beijing, 154–
411 156, 2004.
412 CMA: Sand-dust weather almanac 2008, China Meteorological Press, Beijing, 10-64, 2009.
413 CMA: Sand-dust weather almanac 2009, China Meteorological Press, Beijing, 11-59, 2010.
414 CMA: Sand-dust weather almanac 2010, China Meteorological Press, Beijing, 11-79, 2012.
415 CMA: Sand-dust weather almanac 2011, China Meteorological Press, Beijing, 10-53, 2013.
416 Creamean, J. M., Suski, K. J., Rosenfeld, D., Cazorla, A., DeMott, P. J., Sullivan, R. C., White, A. B.,
417 Ralph, F. M., Minnis, P., Comstock, J. M., Tomlinson, J. M., Prather, K. A.: Dust and Biological
418 Aerosols from the Sahara and Asia Influence Precipitation in the Western U.S., Science, 339,
419 1572-1578, 2013.
420 Cui, W. L.: Chemical transformation of dust components and mixing mechanisms of dust with
421 pollution aerosols during the long range transport from north to south China, M.S. thesis,
422 Department of Environmental Science and Engineering, Fudan University, China, 38 pp., 2009.
423 Dai, Y.J.: Vertical distribution of characteristics of dust aerosols in the near-surface in hinterland of
424 Taklimakan Desert, M.S. thesis, College of Resources and Environmental Science, Xinjiang
425 University, China, 26 pp., 2016.
426 Dentener, F. J., Carmichael, G. R., Zhang, Y., Lelieveld, J., and Crutzen, P. J.: Role of mineral aerosol
427 as a reactive surface in the global troposphere, J. Geophys. Res-Atmos., 101, 22869-22889, 1996.
428 Duce, R. A., LaRoche, J.,Altieri, K., Arrigo, K. R., Baker, A. R., Capone, D. G., Cornell, S., Dentener,
429 F., Galloway, J., Ganeshram, R. S., Geider, R. J., Jickells, T., Kuypers, M. M., Langlois, R., Liss, P.
430 S., Liu, S. M., Middelburg, J. J., Moore, C. M., Nickovic, S., Oschlies, A., Pedersen, T., Prospero, J.,
431 Schlitzer, R., Seitzinger, S., Sorensen, L. L., Uematsu, M., Ulloa, O., Voss, M., Ward, B., and
432 Zamora, L.: Impacts of atmospheric anthropogenic nitrogen on the open ocean, Science, 320,
433 893-897, 2008.
434 Duce, R. A., Liss, P. S., Merrill, J. T., Atlas, E. L., Buat-Menard, P., Hicks, B. B., Miller, J. M.,
435 Prospero, J. M., Arimoto, R., Church, T. M., Ellis, W., Galloway, J. N., Hansen, L., Jickells, T. D.,
436 Knap, A. H., Reinhardt, K. H., Schneider, B., Soudine, A., Tokos, J. J., Tsunogai, S., Wollast, R., and
437 Zhou, M. Y.: The atmospheric input of trace species to the world ocean, Global. Biogeochem. Cy., 5,
438 193-259, 1991.
439 Echeveste, P., Agustí, S., and Tovar-Sánchez, A.: Toxic thresholds of cadmium and lead to oceanic
440 phytoplankton: cell size and ocean basin-dependent effects, Environ. Toxicol. Chem., 31, 1887-1894,
441 2012.
442 Fitzgerald, E., Ault, A. P., Zauscher, M. D., Mayol-Bracero, O. L., and Prather, K. A.: Comparison of
443 the mixing state of long-range transported Asian and African mineral dust, Atmos. Environ., 115,
444 19-25, 2015.
445 Formenti, P., Schütz's, L., Balkanski, Y., Desboeufs, K., Ebert, M., Kandler, K., Petzold, A., Scheuvens,
446 D., Weinbruch, S., and Zhang, D.: Recent progress in understanding physical and chemical
447 properties of African and Asian mineral dust, Atmos. Chem. Phys., 11, 8231–8256, 2011.
448 Fu, X., Wang, S. X., Cheng, Z., Xing, J., Zhao, B., Wang, J. D., and Hao, J. M.: Source, transport and
449 impacts of a heavy dust event in the Yangtze River Delta, China, in 2011, Atmos. Chem. Phys., 14,

1239-1254, 2014.
Gangwar, J. N., Gupta, T., and Agarwal, A.K.: Composition and comparative toxicity of particulate matter emitted from a diesel and biodiesel fuelled CRDI engine, Atmos. Environ., 46, 472-481, 2012.
Grice, S., Stedman, J., Kent, A., Hobson, M., Norris, J., Abbott, J., and Cooke, S.: Recent trends and projections of primary NO_2 emissions in Europe, Atmos. Environ., 43, 2154-2167, 2009.
Guo, C., Yu, J., Ho, T. Y., Wang, L., Song, S., Kong, L., and Liu, H.: Dynamics of phytoplankton community structure in the South China Sea in response to the East Asian aerosol input, Biogeosciences, 9, 1519-1536, 2012.
Han, X., Ge, C., Tao, J. H., Zhang, M. G., and Zhang, R. J.: Air quality modeling for of a strong dust event in east Asia in march 2010, Aerosol. Air. Qual. Res., 12, 615-628, 2012.
Huang, K., Zhuang, G., Li, J., Wang, Q., Sun, Y., Lin Y., and Fu J. S.: Mixing of Asian dust with pollution aerosol and the transformation of aerosol components during the dust storm over China in spring 2007, J. Geophys. Res-Atmos, 115, D00k13, Doi:10.1029/2009jd013145, 2010.
Hwang, H. and Ro, C. U.: Direct observation of nitrate and sulfate formations from mineral dust and sea-salts using low-Z particle electron probe X-ray microanalysis, Atmos. Environ., 40, 3869-3880, 2006.
Hwang, H., Kim, H. K., and Ro, C. U.: Single-particle characterization of aerosol samples collected before and during an Asian dust storm in Chuncheon, Korea, Atmos. Environ., 42, 8738–8746, 2008.
Jickells, T. D., An, Z. S., Andersen, K. K., Baker, A. R., Bergametti, G., Brooks, N., Cao, J. J., Boyd, P. W., Duce, R. A., Hunter, K., Kawahata, H., Kubilay, N., laRoche, J.,Liss, P. S., Mahowald, N., Prospero, J. M., Ridgwell, A. J., Tegen, I., and Torres, R.: Global iron connections between desert dust, ocean biogeochemistry, and climate, Science, 308, 67-71, 2005.
Kang, E., Han, J., Lee, M., Lee, G., and Kim, J. C.: Chemical characteristics of size-resolved aerosols from Asian dust and haze episode in Seoul Metropolitan City, Atmos. Res., 127, 34-46, 2013.
Lee, Y. G., Ho, C., Kim, J., and Kim, J.: Quiescence of Asian dust events in South Korea and Japan during 2012 spring: Dust outbreaks and transports, Atmos. Environ., 114, 92-101, 2015.
Li, W. J., Shao, L. Y., Shi, Z. B., Chen, J. M., Yang, L. X., Yuan, Q., Yan, C., Zhang, X. Y., Wang, Y. Q., Sun, J. Y., Zhang, Y, M., Shen, X. J., Wang, Z. F., and Wang, W. X.: Mixing state and hygroscopicity of dust and haze particles before leaving Asian continent, J. Geophys. Res-Atmos., 119, 1044–1059, 2014.
Lin, X. H., Liu, C. L., and Zhang, H.: Determination of Metal Elements in Aerosol by ICP-AES, Rock & Mineral Analysis, 17, 143-146, 1998.
Liu, L., Zhang, X. Y., Xu, W., Liu, X. J., Li, Y., Lu, X. H., Zhang, Y. H., and Zhang, W. T.: Temporal characteristics of atmospheric ammonia and nitrogen dioxide over China based on emission data, satellite observations and atmospheric transport modeling since 1980, Atmos. Chem. Phys., 106, 1-32, 2017.
Liu, Q. Y., and Bei, Y. L.: Impacts of crystal metal on secondary aliphatic amine aerosol formation during dust storm episodes in Beijing, Atmos. Environ., 128, 227-334, 2016.
Liu, Q. Y., Liu, Y. J., Yin, J. X., Zhang, M. G., and Zhang, T. T.: Chemical characteristics and source apportionment of PM 10 during Asian dust storm and non-dust storm days in Beijing, Atmos. Environ., 91, 85-94, 2014.
Liu, X. H., Zhang, Y., Cheng, S. H., Xing, J., Zhang, Q., Streets, D. G., Jang, C., Wang, W. X., and Hao, J. M.: Understanding of regional air pollution over China using CMAQ, part I performance

evaluation and seasonal variation, Atmos. Environ., 44, 2415-2426, 2010a.
Liu, X. H., Zhang, Y., Xing, J., Zhang, Q., Wang, K., Streets, D. G., Jang, C., Wang, W. X., and Hao, J. M.: Understanding of regional air pollution over China using CMAQ, part II. Process analysis and sensitivity of ozone and particulate matter to precursor emissions, Atmos. Environ., 44, 3719-3727, 2010b.
Liu, Y., Zhang, T. R., Shi, J. H., Gao, H. W., and Yao, X. H.: Responses of chlorophyll a to added nutrients, Asian dust, and rainwater in an oligotrophic zone of the Yellow Sea: Implications for promotion and inhibition effects in an incubation experiment, J. Geophys. Res-Biogeo., 118, 1763-1772, 2013.
Ma, Q. X., Liu, Y. C., Liu, C., Ma, J. Z., and He, H.: A case study of Asian dust storm particles: Chemical composition, reactivity to SO_2 and hygroscopic properties, J. Environ. Sci., 24, 62-71, 2012.
Mori, I., Nishikawa, M., Tanimura, T., and Quan, H.: Change in size distribution and chemical composition of kosa (Asian dust) aerosol during long-range transport, Atmos. Environ., 37, 4253-4263, 2003.
Niu, S. J., and Zhang, C. C.: Researches on sand aerosol chemical composition and enrichment factor in the spring at Helan Mountain area, Journal of Desert Research, 20, 264-268, 2000.
Ohara, T., Akimoto, H., Kurokawa, J., Horii, N., Yamaji, K., Yan, X., and Hayasaka, T.: An Asian emission inventory of anthropogenic emission sources for the period 1980-2020, Atmos. Chem. Phys., 7, 4419-4444, 2007.
Paatero, P., and Tapper, U.: Analysis of different modes of factor analysis as least squares fit problems, Chemometr. Intell. Lab., 18, 183-194, 1993.
Paatero, P.: Least squares formulation of robust non-negative factor analysis, Chemometr. Intell. Lab., 37, 23-35, 1997.
Penrod, A., Zhang, Y., Wang, K., Wu, S. Y. and Leung, L. R.: Impacts of future climate and emission changes on U.S. air quality, Atmos. Environ., 89, 533-547, 2014.
Qi, J. H., Gao, H. W., Yu, L. M., and Qiao, J. J.: Distribution of inorganic nitrogen-containing species in atmospheric particles from an island in the Yellow Sea, Atmos. Res., 101, 938-955, 2011.
Qi, J. H., Li, P. L., Li, X. G., Feng, L. J., and Zhang, M. P.: Estimation of dry deposition fluxes of particulate species to the water surface in the Qingdao area, using a model and surrogate surfaces, Atmos. Environ., 39, 2081-2088, 2005.
Qi, J. H., Shi, J. H., Gao, H. W., and Sun, Z.: Atmospheric dry and wet deposition of nitrogen species and its implication for primary productivity in coastal region of the Yellow Sea, China, Atmos. Environ., 81, 600-608, 2013.
Sheng, Y., Yang, S., Han, Y., Zheng, Q., and Fang, X.: The concentrations and sources of nitrate in aerosol over Dolmud, Qinghai, China, Journal of Desert Research,36, 792-797, 2016.
Shi, J. H., Gao, H. W., Zhang, J., Tan, S. C., Ren, J. L., Liu, C. G., Liu, Y., and Yao, X. H.: Examination of causative link between a spring bloom and dry/wet deposition of Asian dust in the Yellow Sea, China, J. Geophys. Res-Atmos., 117, 127-135, 2012.
Shi, J. H., Zhang, J., Gao, H. W., Tan, S. C., Yao, X. H., and Ren, J. L.: Concentration, solubility and deposition flux of atmospheric particulate nutrients over the Yellow Sea, Deep-sea. Res. Pt. II, 97, 43-50, 2013.
Skjøth C. A., and Hertel, O.: Ammonia Emissions in Europe, Urban Air Quality in Europe, Springer Berlin Heidelberg, The Handbook of Environmental Chemistry, Germany, 163 pp., 2013.

Su, X., Wang, Q., Li, Z., Calvello, M., Esposito, F., Pavese, G., Lin, M., Cao, J., Zhou, C., Li, D., and Xu, H.: Regional transport of anthropogenic pollution and dust aerosols in spring to Tianjin — A coastal megacity in China, Sci. Total. Environ., 584-585, 381-392, 2017.

Tan, S. C., and Wang, H.: The transport and deposition of dust and its impact on phytoplankton growth in the Yellow Sea, Atmos. Environ., 99, 491-499, 2014.

Taylor, S. R.: Abundance of chemical elements in the continental crust: a new table, Geochim. Cosmochim. Ac., 28, 1273-1285, 1964.

Tobo, Y., Zhang, D. Z., Matsuki, A., and Iwasaka, Y.: Asian dust particles converted into aqueous droplets under remote marine atmospheric conditions, PNAS Proceedings of the National Academy of Sciences of the United States of America, 107, 17905–17910, 2010.

U. S., EPA.: Method 1631, Revision E: Mercury in water by oxidation, purge and trap, and cold vapor atomic fluorescence spectrometry, US Environmental Protection Agency Washington, DC, 2002.

Underwood, G. M., Song, C. H., Phadnis, M., Carmichael, G. R., and Grassian, V. H.: Heterogeneous reactions of NO_2 and HNO_3 on oxides and mineral dust: a combined laboratory and modeling study, J. Geophys. Res-Atmos., 106, 18055-18066, 2001.

Uno, I., Eguchi, K., Yumimoto, K., Takemura, T., Shimizu, A., Uematsu, M., Liu, Z., Wang, Z., Hara, Y., and Sugimoto, N.: Asian dust transported one full circuit around the globe, Nat. Geosci., 2, 557-560, 2009.VanCuren, R. A. and Cahill, T. A.: Asian aerosols in North America: Frequency and concentration of fine dust, J. Geophys. Res., 107, 163-176, 2002.

VanCuren, R., and Cahill, T.: Asian aerosols in North America: Frequency and concentration of fine dust, J. Geophys. Res., 107(D24), 4804, doi:10.1029/2002JD002204, 2002.

Walker, J. M., Philip, S., Martin, R. V., and Seinfeld, J. H.: Simulation of nitrate, sulfate, and ammonium aerosols over the United States, Atmos. Chem. Phys., 12, 11213-11227, 2012.

Wang, Z., Pan, X., Uno, I., Li, J., Wang, Z., Chen, X., Fu, P., Yang, T., Kobayashi, H., Shimizu, A., Sugimoto, N., and Yamamoto, S.: Significant impacts of heterogeneous reactions on the chemical composition and mixing state of dust particles: A case study during dust events over northern China, Atmos. Environ., 159, 83-91, 2017a.

Wang, F. J., Chen, Y., Guo, Z. G., Gao, H. W., Mackey, K. R., Yao, X. H., Zhuang, G. S. and Paytan, A.: Combined effects of iron and copper from atmospheric dry deposition on ocean productivity, Geophys. Res. Lett., 44, 2546-2555, 2017b.

Wang, L., Du, H. H., Chen, J. M., Zhang, M., Huang, X. Y., Tan, H. B., Kong, L. D., and Geng, F. H.: Consecutive transport of anthropogenic air masses and dust storm plume: Two case events at Shanghai, China, Atmos. Res., 127, 22-33, 2013.

Wang, Q. Z., Zhuang, G. S., Huang, K., Liu, T. N., Lin, Y. F., Deng, C. R., Fu, Q. Y., Fu, J. S., Chen, J. K., Zhang, W. J., and Yiming, M.: Evolution of particulate sulfate and nitrate along the Asian dust pathway: Secondary transformation and primary pollutants via long-range transport, Atmos. Res., 169, 86-95, 2016.

Wang, Q. Z., Zhuang, G. S., Li, J., Huang, K., Zhang, R., Jiang, Y. L., Lin, Y. F., and Fu, J. S.: Mixing of dust with pollution on the transport path of Asian dust - Revealed from the aerosol over Yulin, the north edge of Loess Plateau, Sci. Total. Environ., 409, 573-581, 2011.

Wang, Y. Q., Zhang, X. Y., and Draxler, R. R.: TrajStat: GIS-based software that uses various trajectory statistical analysis methods to identify potential sources from long-term air pollution measurement data, Environ. Modell. Softw., 24, 938-939, 2009.

Wang, Y. Q., Zhang, X. Y., Gong, S. L., Zhou, C. H., Hu, X. Q., Liu, H. L., Niu, T., and Yang, Y. Q.:

582 Surface observation of sand and dust storm in East Asia and its application in CUACE/Dust, Atmos.
583 Chem. Phys., 8, 545-553, 2008.
584 Wang, Z., Pan, X. L., Uno, I., Li, J., Wang, Z. F., Chen, X. S., Fu, P. Q., Yang, T., Kobayashi, H.,
585 Shimizu, A., Sugimoto, N., and Yamamoto, S.: Significant impacts of heterogeneous reactions on the
586 chemical composition and mixing state of dust particles: A case study during dust events over
587 northern China, Atmos. Environ., 159, 83-91, 2017.
588 Williams, R. W.: A model for the dry deposition of particles to natural water surface, Atmos. Environ.,
589 16, 1933-1938, 1982.
590 Wu, F., Zhang, D. Z., Cao, J. J., Guo, X., Xia, Y., Zhang, T., Lu, H., and Cheng, Y.: Limited production
591 of sulfate and nitrate on front-associated dust storm particles moving from desert to distant populated
592 areas in northwestern China, Atmos. Chem. Phys., 853, 1-22, 2016.
593 Xin, W. C., Lin, X. H., and Xu, L.: ICP-MS Determination of 34 trace elements in marine sediments,
594 Physical Testing and Chemical Analysis (Part B: Chemical Analysis), 4, 29, 2012.
595 Xu, J. Z., Wang, Z. B., Yu, G. M., Qin, X., Ren, J. W., and Qin, D. H.: Characteristics of water soluble
596 ionic species in fine particles from a high altitude site on the northern boundary of Tibetan Plateau:
597 Mixture of mineral dust and anthropogenic aerosol, Atmos. Res., 143, 43-56, 2014.
598 Yang, D. Z., Wang, C., Wen, Y. P., Yu, X. L., and Xiu, X. B.: Analysis of Two Sand Storms In Spring
599 1990, Quarterly Journal of Applied Meteorology, 6, 18-26, 1995.
600 Yang, D. Z., Yan, P., and Xu, X. D.: Characteristics of aerosols under dust and sand weather in Beijing,
601 Quarterly Journal of Applied Meteorology, 1, 185-194, 2002.
602 Yao, X. H., and Zhang, L.: Supermicron modes of ammonium ions related to fog in rural atmosphere,
603 Atmos. Chem. Phys., 12, 11165-11178, 2012.
604 Yao, X. H., Lau, A. S., Fang, M., Chan, C., and Hu, M.: Size Distributions and Formation of Ionic
605 Species in Atmospheric Particulate Pollutants in Beijing, China: 1—Inorganic Ions. Atmos. Environ.,
606 37, 2991-3000, 2003.
607 Zhang, G. S., Zhang, J., and Liu, S. M.: Characterization of nutrients in the atmospheric wet and dry
608 deposition observed at the two monitoring sites over Yellow Sea and East China Sea, J. Atmos.
609 Chem., 57, 42-57, 2007.
610 Zhang, J., Zhang, G. S., Bi, Y. F., and Liu, S. M.: Nitrogen species in rainwater and aerosols of the
611 Yellow and East China seas: Effects of the East Asian monsoon and anthropogenic emissions and
612 relevance for the NW Pacific Ocean, Global Biogeochem. Cy., 25, 113-120, 2011.
613 Zhang, K., and Gao, H. W.: The characteristics of Asian-dust storms during 2000–2002: From the
614 source to the sea, Atmos. Environ., 41, 9136-9145, 2007.
615 Zhang, Q., Streets, D. G., Carmichael, G. R., He, K. B., Huo, H., Kannari, A., Klimont,Z., Park, I. S.,
616 Reddy, S., Fu, J. S., Chen, D., Duan, L., Lei, Y., Wang, L. T., and Yao, Z. L.: Asian emissions in 2006
617 for the NASA INTEX-B mission. Atmos. Chem. Phys., 9, 5131-5153, 2009.
618 Zhang, W. J., Zhuang, G. S., Huang, K., Li, J., Zhang, R., Wang, Q. Z., Sun, Y. L., Fu, J. S., Chen, Y.,
619 and Xu, D. Q.: Mixing and transformation of Asian dust with pollution in the two dust storms over
620 the northern China in 2006, Atmos. Environ., 44, 3394-3403, 2010a.
621 Zhang, Y. and Carmichael, G. R.: The role of mineral aerosol in tropospheric chemistry in East Asia - a
622 model study, J. Appl. Meteorol., 38, 353-366, 1999.
623 Zhang, Y., Sunwoo, Y., Kotamarthi, V. R., and Carmichael, G. R.: Photochemical oxidant processes in
624 the presence of dust: an evaluation of the impact of dust on particulate nitrate and ozone formation, J.
625 Appl. Meteorol., 33, 813-824, 1994.

Zhang, Y., Yu, Q., Ma, W. C., and Chen, L. M.: Atmospheric deposition of inorganic nitrogen to the eastern China seas and its implications to marine biogeochemistry, J. Geophys. Res-Atmos., 115, 3421-3423, 2010b.

670 **Table 1**. Sampling information for the aerosol samples collected at the Baguanshan site in the coastal
671 region of the Yellow Sea.

Sampling year	Sample category	Sampling number	Sampling time	Weather characteristics
2008	Samples on dust days	20080301	From 13:22 a.m. to 17:22 p.m. on Mar. 1st	Floating dust[a]
		20080315	From 13:21 a.m. to 17:21 p.m. on Mar. 15th	Floating dust
		20080425	From 13:14 a.m. to 17:14 p.m. on Apr. 25th	Floating dust
		20080528	From 11:38 a.m. to 15:38 p.m. on May 28th	Floating dust
		20080529	From 10:15 a.m. to 12:15 p. m. on May 29th[b]	Floating dust
	Samples on non-dust days	20080316	From 13:00 a.m. to 17:00 p.m. on Mar. 16th	Sunny day
		20080424	From 13:00 a.m. to 17:00 p.m. on Apr. 24th	Sunny day
		20080522	From 13:00 a.m. to 17:00 p.m. on May 22nd	Cloudy day with mist
2009	Samples on dust days	20090316	From 8:25 a.m. to 12:25 p.m. on Mar. 16th	Floating dust
	Samples on non-dust days	20090306	From 13:00 a.m.to 17:00 p.m. on Mar. 6th	Sunny day
2010	Samples on dust days	20100315	From 11:30 a.m.to 15:30 p.m. on Mar. 16th	Mist after floating dust
		20100320	From 10:30 a.m. to 14:30 p.m. on Mar. 20th	Floating dust
		20100321	From 10:30 a.m. to 14:30 p.m. on Mar. 21st	Floating dust
	Samples on non-dust days	20100324	From 11:30 a.m. to 15:30 p.m. on Mar. 24th	Sunny day
2011	Samples on dust days	20110319	From 12:00 a.m. to 16:00 p.m. on Mar. 19th	Floating dust
		20110415	From 12:00 a.m. to 16:00 p.m. on Apr. 15th	Floating dust
		20110418	From 12:25 a.m. to 16:25 p.m. on Apr. 18th	Floating dust[c]
		20110501	From 12:10 a.m. to 16:10 p.m. on May 1st	Floating dust
		20110502	From 16:00 a.m. to 20:00 p.m. on May 2nd	Floating dust
	Samples on non-dust days	20110308	From 12:00 a.m. to 16:00 p.m. on Mar. 8th	Sunny day

	20110416	From 12:00 a.m. to 16:00 p.m. on Apr. 16th	Sunny day
	20110523	From 12:00 a.m. to 16:00 p.m. on May 23rd	Sunny day

[a]Note that one exterior dust sample was collected on March 1 when no dust was recorded by the MICAPS. However, the MICAPS information indeed showed dust events in China on March 1. The modeled spatial distribution of the PM_{10} mass concentration for this dust event on March 1 implies that the sample should be classified as a dust sample. The supporting figures are shown in Fig. S1.

[b]The sampling duration was reduced to only 2 hrs because of extremely high particle loads. In addition, the samples with IDs of 20080528 and 20080529 were subjected to two different dust events occurring over two days instead of continuous samples for one dust event (CMA, 2009).

[c]Note that one exterior dust sample was collected on April 18when no dust was recorded by the MICAPS. However, blowing dust occurred and was recorded on April 17 by the Sand-dust Weather Almanac 2011 (CMA, 2013). The modeled spatial distribution of the PM_{10} mass concentration for this dust event on April 18 implies that the sample should be classified as a dust sample. The supporting figure is Fig. S2.

712 **Table 2.** Detection limits, precisions and recoveries of water-soluble ions and metal elements.

Component	Measurement method	Detection limit ($\mu g\ L^{-1}$)	Precision (RSD%)	Recovery (%)
NO_3^-	IC	2.72	1.54	97
SO_4^{2-}		1.62	1.55	98
NH_4^+		0.4	1.10	97
Ca^{2+}		0.44	0.79	94
Cu	ICP-MS (Xin et al., 2012)	0.006	4.0	106
Zn		0.009	2.5	102
Cr		0.004	3.0	95
Sc		0.002	2.4	97
Pb		0.008	3.9	104
Al	ICP-AES (Lin et al., 1998)	7.9	0.6	103
Ca		5.0	1.2	99
Fe		2.6	0.7	104
Na		3.0	0.6	99
Mg		0.6	0.6	105
Hg	CVAFS	0.0001	6.6	105
As	CVAFS	0.1	5.0	98

713
714
715
716
717
718
719
720
721
722
723
724
725
726
727
728
729
730
731
732
733
734
735
736
737

738 **Table 3.** The average concentrations and EFs of metal elements on dust and non-dust days.

Element	Concentration (ng/m^3)		EF*	
	Non-dust days	Dust days	Non-dust days	Dust days
Sc	1.11	13.90	-	-
Al	8.53×10^3	6.86×10^4	3.8	1.4
Fe	4.91×10^3	3.88×10^4	3.	1.2
Ca	1.05×10^4	4.29×10^4	14.0	2.1
Mg	1.62×10^3	1.58×10^4	3.5	1.1
Cu	50.2	124.5	36.3	6.1
Pb	127.9	221.0	389.4	56.1
Zn	340.0	457.7	248.9	20.6
Cr	33.8	244.0	44.0	11.1
Hg	0.26	0.36	176.0	13.8
As	25.5	27.4	707.2	43.9

739 *EF values less than 10 indicate that the studied element is mainly derived from crustal sources,
740 whereas EF values much higher than 10 indicate an anthropogenic source.
741
742
743
744
745
746
747
748
749
750
751
752
753
754
755
756
757
758
759
760
761
762
763
764
765
766
767
768

Table 4. Average concentrations of inorganic nitrogen (DIN), TSP, NOx, relative humidity (RH) and air temperature for each aerosol sample category in Qingdao.

	Sample number	TSP ($\mu g \cdot m^{-3}$)	NO_3^- ($\mu g \cdot m^{-3}$)	NH_4^+ ($\mu g \cdot m^{-3}$)	RH (%)	T (℃)	NOx ($\mu g \cdot m^{-3}$)	Summary
Category 1	20080301	527	20.5	12.7	57	7.0	36	DIN concentration on dust days higher than that on non-dust days
	20080315	410	19. 5	29.9	62	11.0	59	
	20090316	688	15.9	17.2	27	16.0	75	
	20100321	519	16.5	9.4	51	8.8	76	
	20110502	810	21.0	11.0	49	17.7	62	
Category 2	20080425	622	6.8	2.0	30	18.0	40	DIN concentration on dust days lower than that on non-dust days
	20080528	2579	9.2	2.7	17	27.0	34	
	20080529	2314	17.5	4.8	60	20.0	29	
	20110319	939	12.3	9.4	16	12.6	93	
	20110501	502	4.5	5.3	23	21.6	66	
Category 3	20100315	501	5.4	4.3	30	7.2	73	NO_3^- concentration on dust days lower than that on non-dust days; NH_4^+ close to that on non-dust days
	20100320	3857	5.5	3.4	35	10.6	92	
	20110418	558	3.8	6.6	33	12.6	47	
Non-dust [a]	20080316	225	12.6	8.4	28	11.0	60	
	20080424	137	21.7	7.2	49	18.0	53	
	20080522	206	27.4	16.6	78	20.0	60	
	20090306	94	2.9	3.0	29	7.00	51	
	20100324	275	7.2	2.4	23	9.0	82	
	20110308	194	13.0	13.1	20	11.5	111	
	20110416	252	5.6	5.4	26	14.1	55	
	20110523	224	15.2	10.2	42	20.6	49	

[a]For the corresponding non-dust day for each dust event, see Table 1.

775 **Table 5.** Comparison of the inorganic nitrogen (DIN) content in sand and aerosol particles on dust days
776 or close to the dust source region (unit: μg/g).

Sands sampled in dust source regions			Aerosols in or close to dust source region on dust days			Aerosols in the coastal region of the Yellow Sea	
Study region and data source	Relative concentration[a]		Study region and data source	Relative concentration[a]			
	NO_3^-	NH_4^+		NO_3^-	NH_4^+	NO_3^-	NH_4^+
Zhurihe (This study)	25.46 ± 22.87	4.21 ± 1.03	Duolun (Cui, 2009)	1200	900	Non-dust: 28,200 ±24,819	Non-dust: 24,063 ±21,515
Alxa Left Banner, Inner Mongolia (Niu and Zhang, 2000)	62.1 ±7.4	79.1 ±1.1	Alxa Right Banner, Inner Mongolia (Niu and Zhang, 2000)	1975[b]	4091[b]	Category 1: 34,892 ±9570	Category 1: 22,571 ±7,016
Yanchi, Ningxia (Niu and Zhang, 2000)	46.4 ±2.2	80.9 ±1.3	Hinterland of the Taklimakan Desert, Xinjiang (Dai et al., 2016)	142-233	2-15	Category 2: 5,542 ±5,117	Category 2: 4,758 ±5,698
			Average of Sonid Youqi, Huade (Inner Mongolia), Zhangbei (Hebei) (Mori et al., 2003)	253	710	Category 3: 6,359 ±4,697	Category 3: 7,059 ±5,591
			Yulin, the north edge of Loess Plateau (Wang et al., 2011)	216.4	80.6		
			Golmud, Qinghai(Sheng et al., 2016)	892.9	-[c]		
			Hohhot, Inner Mongolia (Yang et al., 1995)	588.1	No data		

777 [a]Relative concentration of DIN per aerosol particle mass
778 [b]Samples collected on a floating dust day (horizontal visibility less than 10000 m and very low wind
779 speed)
780 [c]The ammonium concentration was lower than the detection limit of the analytical instrument.
781
782
783
784

Table 6. Sources and source contributions (expressed in%) calculated for aerosol samples collected during dust and non-dust events

Dust event		Comparison days	
Source	% of TSP	Source	% of TSP
Soil dust	36	Soil dust	23
Industrial	21	Industrial	24
Secondary aerosol	6	Secondary aerosol	23
Oil combustion	6	Biomass burning	16
Coal combustion and other uncertain sources	31	Coal combustion	5
		Sea salt	9

Table 7. Concentrations of TSP, NO_3^-, and NH_4^+; transport speed; transport distance over the sea; transport distance; air temperature; RH; average mixed layer during transport and transport time in polluted region for atmospheric aerosol samples on dust days.

Group	Sample number	TSP ($\mu g/m^3$)	NO_3^- ($\mu g/g$)	NH_4^+ ($\mu g/g$)	Speed (km/h)	Distance over the sea (km)	Transport altitude (m)	Mixed layer depth (m)	R-time[a] (h)	T[b] (℃)	RH[c] (%)
Category 1 IN>ND	080301	527	38,984	24,107	40.1	0	1,160±702	864±745	39	-2.9±11.7	29±10
	080315	410	47,611	34,130	79.1	0	4,921±1,870	950±525	13	-32.5± 16.4	34±16
	090316	688	23,050	25,012	86.2	0	3,739±1083	702±665	11	-19.1±11.7	42±17
	100321	519	31,741	18,155	87.2	0	3,407±1,249	1,113±760	19	-23.0±13.6	42±22
	110502	810	25,995	13,632	30.2	177	3,666±1,371	747±957	26	-13.2±15.8	31±13
Category 2 IN<ND	080425	256	4,089	372	29.6	0	887±656	1,161±1,040	10	-2.7±6.1	66±13
	080528	2579	232	72	88.2	244	4,336±1461	1,064±830	8	-15.5±13.6	31±16
	080529	2314	26	166	63.7	94	2,148±1,725	1,194±816	43	3.6±18.4	25±17
	110319	939	13,088	10,067	70.6	132	4,271±1867	790±719	27	-26.3±20.0	48±32
	110501	502	8,924	10,631	35.1	252	3,212±810	916±1,114	5	-13.4±8.5	39±13
Category 3 NO_3^-<ND NH_4^+≅ND	100315	501	10,767	8,515	57.3	0	5,009±1410	1,110±365	7	-40.4±13.3	45±29
	100320	3857	1,418	884	76.9	0	1,284±401	525±371	10	-12.2±6.3	61±16
	110418	558	6,891	11,778	35.6	931	1,344±780	695±672	2	-0.1±8.2	52±28

[a]Residence time of the air mass passing over parts of highly polluted regions according to the trajectories of samples.

[b]Average air temperature with the definition in Section 2.4.

[c]Average relative humidity with the definition in Section 2.4.

Table 8. Dry deposition of TSP (mg/m^2/month), particulate inorganic nitrogen (mg N/m^2/month) and some toxic trace metals (mg/m^2/month) on dust and non-dust days.

	Dry deposition flux							
	TSP	NO_3^--N	NH_4^+-N	$N_{NH4++NO3}$-	Fe	Cu	Pb	Zn
Category 1[a]	8,000 ± 1800	65 ±9	24 ±14	90 ±17	533 ±179	2 ±0.3	0.3 ±0.3	6 ±2
Category 2[a]	18000 ± 11,000	13 ±18	8 ±4	21 ±22	1300 ±1000	3 ±2	0.08 ±0.04	4 ±1
Category 3[a]	29,000 ± 31,000	26 ±6	17 ±8	42 ±12	2100 ±2200	6 ±1	0.20 ±0.02	5 ±3
Non-dust	2,800 ± 700	48 ±33	15 ±8	63 ±39	190 ±110	1 ±1	0.09 ±0.1	5 ±4

[a]For the characterization of $N_{NH4++NO3}$- concentration and sample information of the category, see Table 3.

Table 9. Comparison of dry deposition flux and normalized flux of TSP (mg/m^2/month) and $N_{NH4+NO3}$- (mg N/m^2/month) with observations from other studies (mg N/m^2/month)

Source	Year	Area		TSP	$N_{NH4+NO3}$-	Normalized average flux of $N_{NH4+NO3}$-[a]
This work	2008-2011	Qingdao, coastal region of the Yellow Sea	Non-dust day	2,800±700	63±39	93.90
			Dust day	10,138±15,940	58±36	101.39
			Average of dust and non-dust			97.64
Qi et al., 2013	2005-2006	Qingdao, coastal region of the Yellow Sea	Average of nine months samples	159.2 - 3,172.9	1.8-24.5	94.75
Zhang et al., 2011	1997-2005	Qingdao	Average of annual samples		132	99.65
Zhang et al., 2007	1999-2003	The Yellow Sea			11.43	9.91
Shi et al., 2013	2007	The Yellow Sea	Non-dust day		19.2	132.17
			Dust day		104.4	227.07
			Average of dust and non-dust			179.62

[a]The calculation method of the normalized flux of $N_{NH4+NO3}$- was discussed in Section 3.7.

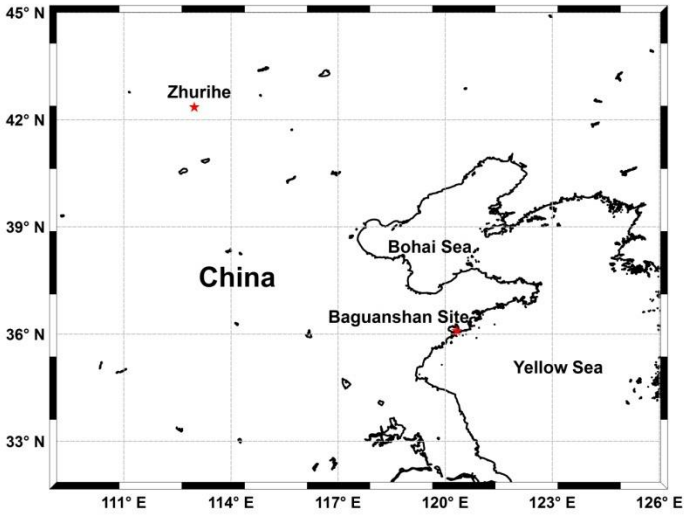

Figure 1. Location of the aerosol and dust sampling sites.

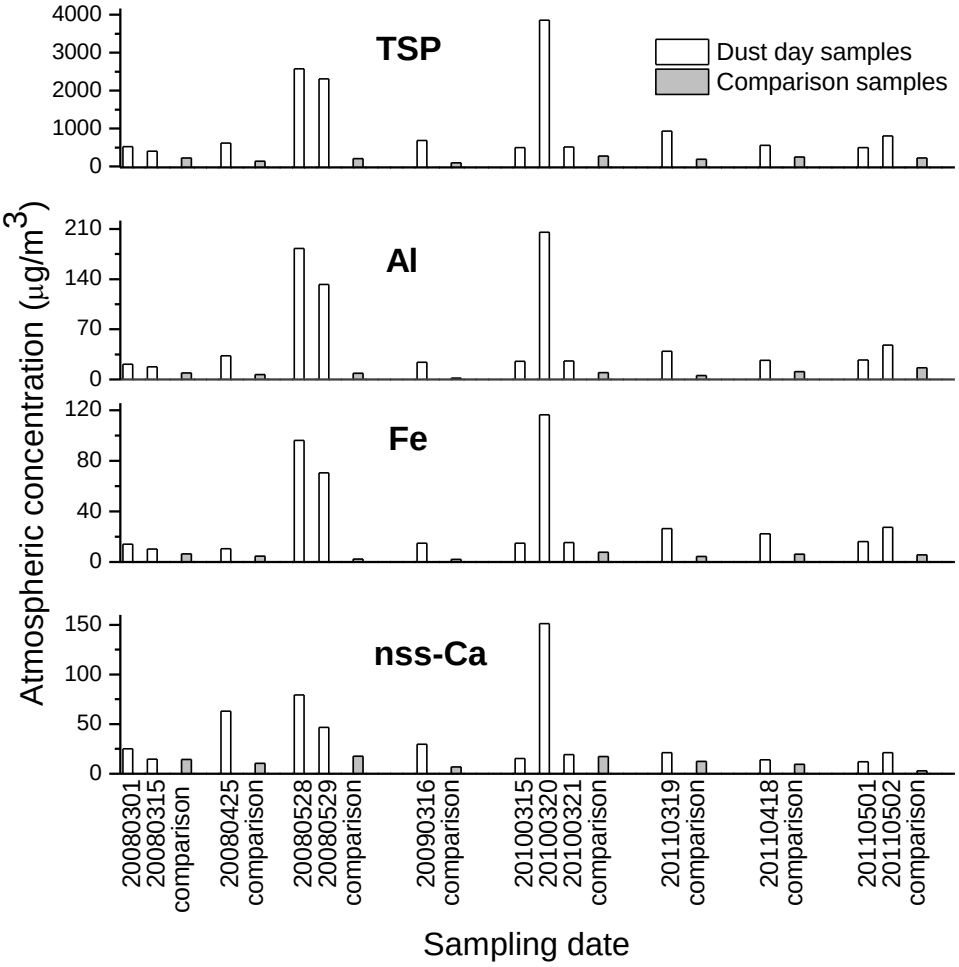

Figure 2. Mass concentrations of TSP, Al, Fe and nss-Ca in aerosol samples collected at the Baguanshan site on dust and comparison days from 2008-2011.

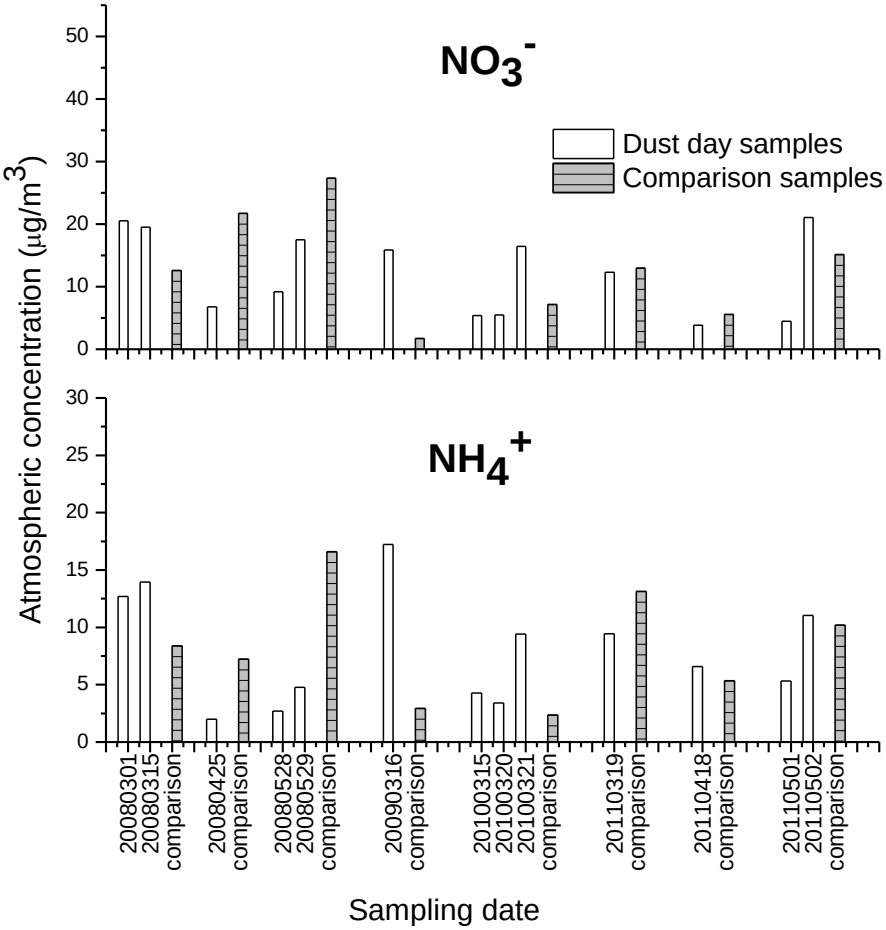

Figure 3. Mass concentrations of NH_4^+ and NO_3^- in aerosol samples collected at the Baguanshan site on dust and comparison days during March-May in 2008 to 2011.

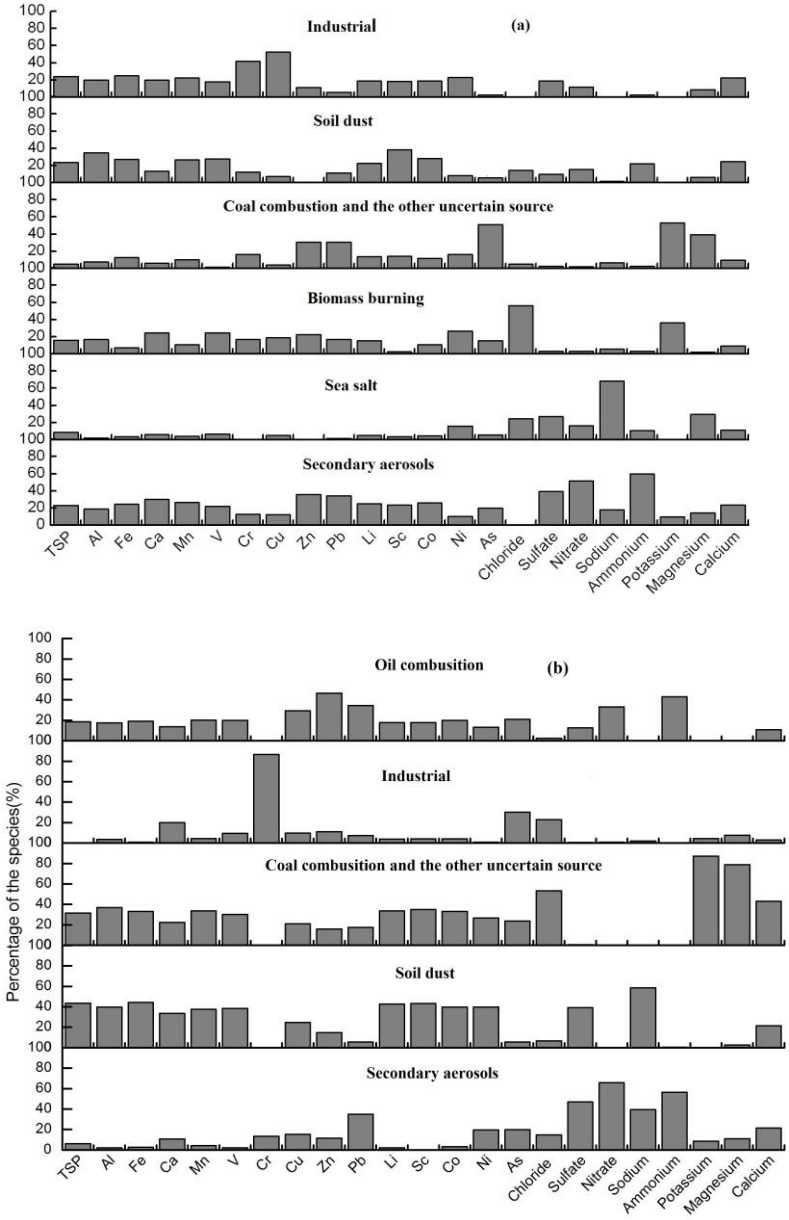

Figure 4. Source profiles of atmospheric aerosol samples collected on non-dust (a) and dust (b) days using the PMF model.

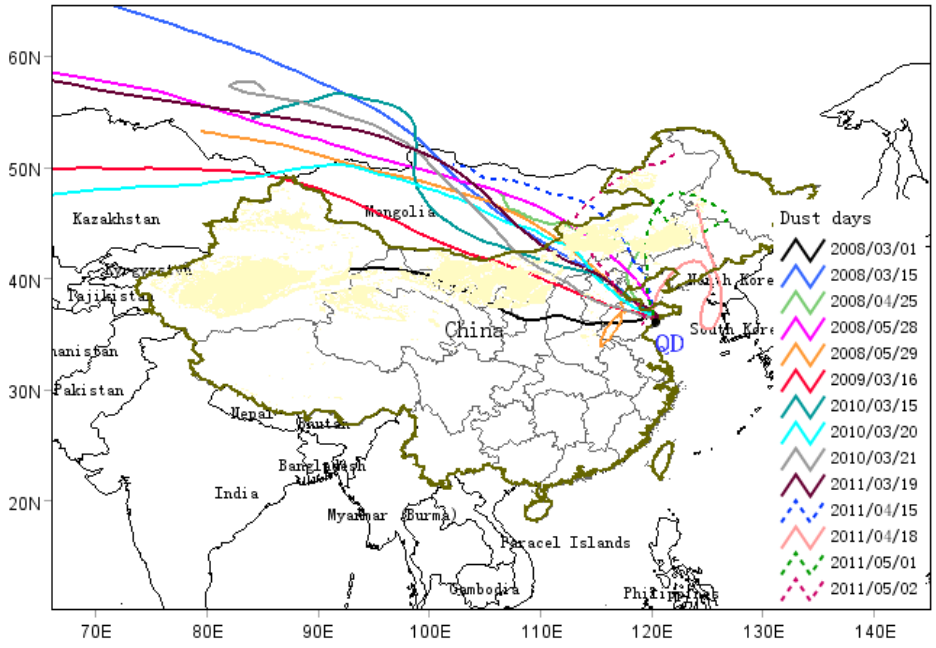

Figure 5. The 72-h backward trajectories for dust samples from 2008 to 2011(the yellow domains in the map represent the dust source regions in China).

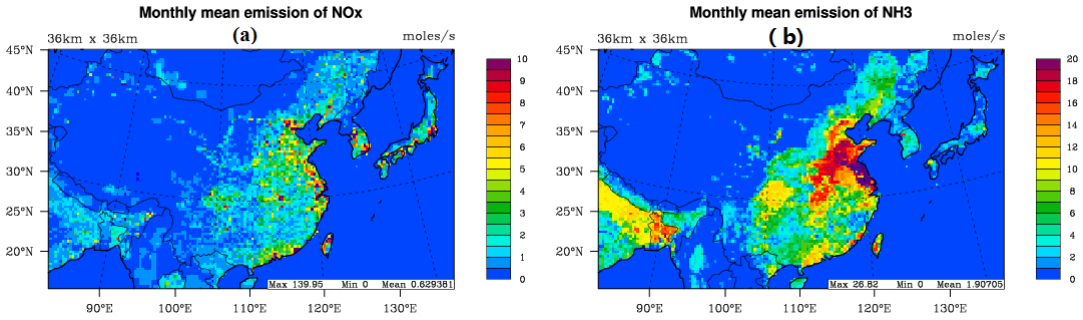

Figure 6. Seasonal mean emissions of NOx (a) and NH_3 (b) over East Asia from March-May 2008.